

## Infrared radiances over the Tibetan plateau as measured by INSAT-1A VHRR in an active monsoon situation

R. R. KELKAR, P. N. KHANNA and SANT PRASAD

India Meteorological Department, New Delhi

(Received 5 January 1983)

सार — 12/13 अगस्त 1982 को भारत पर एक खास किस्म की सक्रिय मानसून स्थिति के लिये इन्सैट-एक (ए) अति उच्च-विकिरण-मापी के आंकड़ों का प्रयोग किया गया था। इससे तिब्बत के पठारी क्षेत्र पर तापमान प्रतिमान का मानचित्र बनाया गया, पठार और आसपास के क्षेत्र पर भूरी छाया तथा अवरोधित विकिरण प्रभा मानों का विश्लेषण किया गया है। गर्म क्षेत्रों के विस्तार में आकाशीय तथा दैनिक प्राचलों तथा मेघाच्छन्नता पर चर्चा की गई है। पठारी क्षेत्र, आस-पास के क्षेत्र की तुलना में अधिक गर्म दिखाया गया है जिससे आरम्भ के सैद्धांतिक तथा अनु-करणीय अध्ययनों में मदद मिलती है।

ABSTRACT. INSAT-1A VHRR data have been used for a typical active monsoon situation over India which prevailed on 12/13 August 1982, to map the temperature pattern over the Tibetan plateau region. Gray shade and IR brightness values are analysed over the plateau and surrounding areas. Spatial and diurnal variations in the extent of the warm area and cloudiness are discussed. The plateau region is shown to be warmer than the surrounding which lends support to earlier theoretical and simulation studies.

### 1. Introduction

It is generally recognised that the Tibetan plateau has a dominant influence on the Asian summer monsoon circulation. Its dual action as a physical obstruction to the lower tropospheric air currents and as an elevated heat source in summer, has been a subject of investigation since long (Academia Sinica 1958, Flohn 1958), even though meteorological data over the region was earlier quite meagre. Koteswaram (1958) proposed a model of the mechanism of the monsoon circulation built around the central idea of the heating of the Tibetan plateau.

Radiative equilibrium studies of the atmosphere along 80° E meridian, using numerical models have confirmed that there is a large net radiative heating over the elevated Himalaya-Tibet region in July (Godbole *et al.* 1970, Kelkar 1970). In a numerical simulation of the Indian summer monsoon, Godbole (1973) found that the simulated temperatures in the upper troposphere were about 4° to 13° K warmer above the Himalayas than those at the same level over the equatorial region. However, without the Himalayas, this temperature difference was reduced to about 1° K.

Analysis of 500 mb level temperatures over the region (Chin and Lai 1974), however, indicates that during the monsoon season, a closed isotherm of 273° K lies over the heart of the Tibetan plateau. The temperature falls southward and is of the order of 267° K over Sri Lanka. To the north of Tibet, the fall is more rapid with temperature of 263° K observed at 45° N latitude.

India's first multipurpose geostationary satellite INSAT-1A which was positioned at 74° E provided a unique opportunity during a short period of its useful life, of observing the data-sparse Tibetan region in the monsoon season of 1982. The limited data acquired from the satellite have been processed at the Meteorological Data Utilisation Centre, New Delhi. A typical case on 12/13 August 1982, when an active monsoon situation prevailed over India, is discussed to illustrate the thermal patterns which existed in the zonal and meridional directions across Tibetan and adjoining regions. It is considered that this preliminary study would demonstrate the utility of INSAT data for studying dynamical aspects of large scale monsoon systems.

### 2. INSAT-VHRR data processing

The Very High Resolution Radiometer (VHRR) on board INSAT-1A has two types of sensors, *viz.*, visible and infrared. The visible sensor measures radiation reflected by the earth's surface and cloud tops in the region 0.55-0.75 $\mu$ . The IR sensor measures energy radiated by the earth-atmosphere system in the 10.5-12.5 $\mu$  region. A full-disc visible image comprises 4096  $\times$  4096 pixels (picture elements) while a full-disc IR image has 1024  $\times$  1024 pixels. At the sub-satellite point a visible pixel corresponds to an area of 2.75 km  $\times$  2.75 km on the earth's surface and an IR pixel to an area of 11 km  $\times$  11 km. It takes about 23 min to complete a full-disc scan.

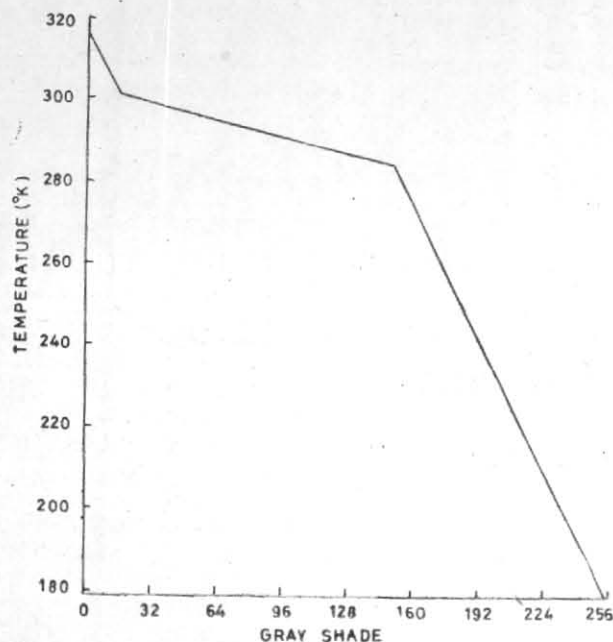


Fig. 1

If we assume the earth's surface or cloud top to behave as a perfect black body and neglect any atmospheric attenuation in the 10.5-12.5  $\mu$  region, the black body temperature can be derived from the IR radiance measured by the VHRR as follows :

$$T_B = C_2 v / \ln (C_1 v^3 / R + 1) \quad (1)$$

where  $T_B$  is the black body temperature in  $^{\circ}\text{K}$  of the earth's surface or cloud top,  $R$  is the radiance in  $\text{Wm}^{-2} \text{sr}^{-1} (\text{cm}^{-1})$ ,  $v$  is the wave number  $= 1/\lambda$ ,  $\lambda$  being the central wavelength 11.5  $\mu$ .  $C_1$  and  $C_2$  are constants having values respectively  $1.1911 \times 10^{-8} \text{ Wm}^{-2} \text{sr}^{-1} (\text{cm}^{-1})^{-1}$  and  $1.439 \text{ }^{\circ}\text{K} (\text{cm}^{-1})^{-1}$ .

Table 1 shows the black body radiances at 11.5  $\mu$  for the various temperatures. Besides conversion to temperatures, the radiances received by the VHRR's IR sensor are also converted to what are known as gray shades. A gray shade of 255 corresponds to a temperature of 179 $^{\circ}$  K and a gray shade of 0 to 317 $^{\circ}$  K. The temperature-gray shade relationship is not linear but has been designed to provide a temperature resolution of about 0.1 $^{\circ}$  K in the range 284-301 $^{\circ}$  K and a resolution of 1 $^{\circ}$  K outside this range (Fig. 1).

In addition to the real time VHRR data processing mentioned above, the Data Analysis and Interactive Display (DAID) system at MDUC, New Delhi, provides many other capabilities for analysis of the data. DAID was used in the present study to obtain computer plots of isopleths of gray shade and temperature over selected image sectors. The software filters out noisy data and also smooths out the contours. Another use made was to obtain information about individual pixel gray shades along straight line segments of an image. This process is termed in the software as 'slicing'. Latitude/longitude grids were super-imposed on the contours by means of the navigation capabilities of DAID.

TABLE 1

Black-body radiances at 11.5  $\mu$  at various temperatures

Temp. ( $^{\circ}\text{K}$ )	Radiance [ $\text{Wm}^{-2} \text{sr}^{-1} (\text{cm}^{-1})^{-1}$ ]	Temp. ( $^{\circ}\text{K}$ )	Radiance [ $\text{Wm}^{-2} \text{sr}^{-1} (\text{cm}^{-1})^{-1}$ ]
180	0.0075	260	0.0642
190	0.0108	270	0.0768
200	0.0150	280	0.0908
210	0.0203	290	0.1062
220	0.0266	300	0.1228
230	0.0341	310	0.1409
240	0.0429	320	0.1602
250	0.0529		

Four INSAT images were selected for the present study, viz., 1200 and 1800 GMT of 12 August 1982 and 0000 and 0600 GMT of 13 August 1982. During this period the monsoon was vigorous over Gujarat region and active over Orissa, coastal Andhra Pradesh, Telangana and coastal Karnataka. The axis of the monsoon trough was passing through Ganganagar, Gwalior and Ambikapur at 0300 GMT of 12 August and shifted southwards appreciably the following day. A monsoon depression was centred at 1200 GMT of 12 August near 20.5 $^{\circ}$  N and 87.5 $^{\circ}$  E. It crossed the north Orissa coast by the next morning.

A sector of INSAT visible image for 0600 GMT of 13 August is reproduced in Fig. 2, from which the cloudy and cloud-free areas can be differentiated. It is seen that the central part of the Tibetan plateau is cloud free and the surface features can be observed clearly.

The four INSAT images were sectorised for the purpose of temperature contouring over an area bounded by 70 $^{\circ}$  E to 105 $^{\circ}$  E longitude and 20 $^{\circ}$  N to 50 $^{\circ}$  N latitude. The temperature contouring was done at intervals of 25 $^{\circ}$  K from 200 $^{\circ}$  to 300 $^{\circ}$  K. For the 0600 GMT image, additional contours for 310 $^{\circ}$  and 315 $^{\circ}$  K were also plotted. For the purpose of slicing a wider area was sectorised. The zonal slice was taken along 32.5 $^{\circ}$  N latitude from 60 $^{\circ}$  to 100 $^{\circ}$  E. The meridional slice was taken along 90 $^{\circ}$  E longitude from 25 $^{\circ}$  to 50 $^{\circ}$  N.

### 3. Results and discussion

#### 3.1. Orography of the Himalaya-Tibet region

What is generally designated as the Tibetan plateau in meteorological literature is actually a region of highly variable terrain. The main plateau lies between 80 $^{\circ}$  to 104 $^{\circ}$  E and 30 $^{\circ}$  to 37 $^{\circ}$  N. The contour for a terrain height of 3 km is shown in Fig. 3. South of the

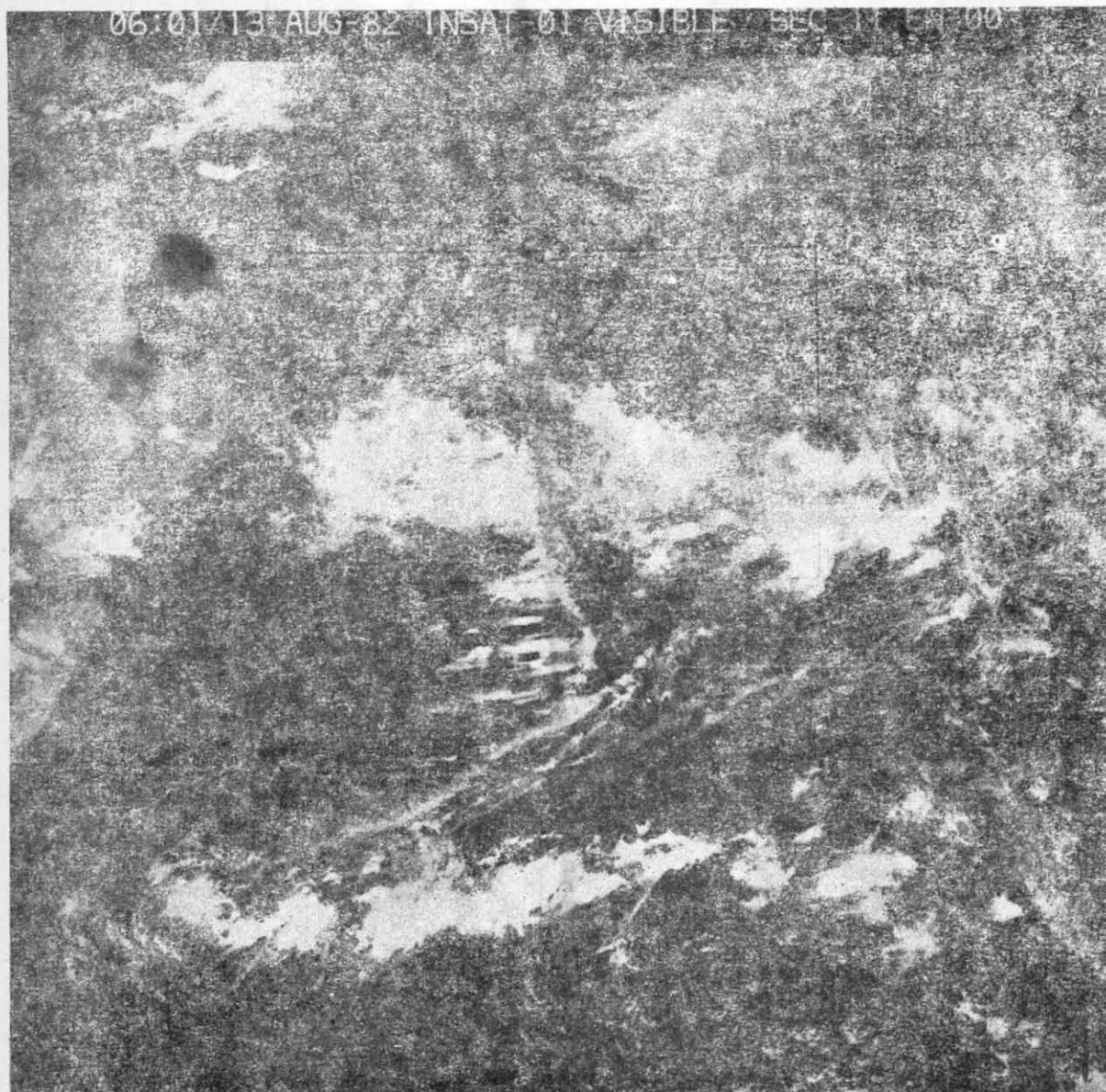


Fig. 2

main plateau runs the Himalaya range with individual peaks rising above 8 to 9 km. The Kunlun range lies to the north of the plateau and further north between  $40^{\circ}$  and  $45^{\circ}$  N lies the Tien Shan range. In between the Tien Shan and Kunlun mountains is the desert of Takla Makan and the Gobi desert is situated to the northeast of the plateau. Tsaidam is a low-lying basin within the plateau region.

### 3.2. Zonal and meridional slices

Figs. 4 and 5 show the pixel-to-pixel variation in gray shade along  $32.5^{\circ}$  N latitude and  $90^{\circ}$  E longitude respectively. In each of the four images selected for this study, the purpose of slicing is to examine the differences in IR radiances over the Tibetan plateau from those over other areas located along the same latitude or longitude and whether these differences can be attri-

buted to topographical features. The zonal slice runs across the Afghanistan plains, the Hindukush mountains, the Indus valley, the Himalayas and the Tibetan plateau. The meridional slice cuts through the Ganges plains, the Himalayas, the Tibetan plateau, Kunlun range, Sinkiang and the Altai range.

Both Figs. 4 and 5 clearly bring out very low gray shade values (10 to 20) at 0600 GMT, *i.e.*, higher temperatures over the central Tibetan plateau ( $86^{\circ}$  to  $91^{\circ}$  E in Fig. 4 and  $30^{\circ}$  to  $34^{\circ}$  N in Fig. 5). In the meridional slice, no other region has such low gray shade values. In the zonal slice, comparable values are observed only over the warm and cloud-free Afghanistan plains ( $60^{\circ}$  to  $67^{\circ}$  E). In Figs. 4 and 5, the pixel-to-pixel variation in gray shade is of particular interest in certain segments, *viz.*,  $67^{\circ}$  to  $72^{\circ}$  E,  $80^{\circ}$  to  $86^{\circ}$  E,  $86^{\circ}$  to  $91^{\circ}$  E,



Fig. 3

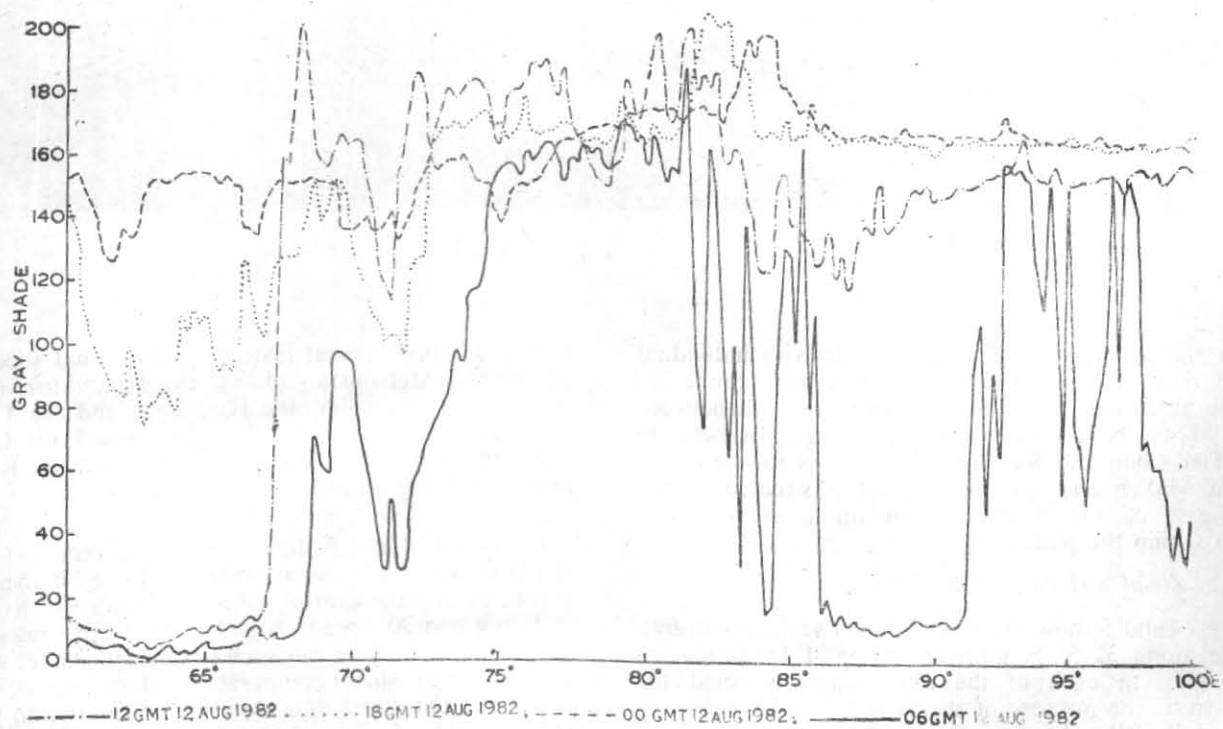


Fig. 4

and 95° to 100° E (in Fig. 4), and 28° to 30° N, 34° to 42° N, and north of 45° N (in Fig. 5). In order to understand these variations, the INSAT cloud pictures (visible and IR) were examined so that the effects of orography and cloud development could be isolated.

**67° to 72° E**— This segment covers the Sulaiman mountain ranges between 67° to 70° E and plain area to the east of 70° E. At 1200 GMT, the presence of convective clouds is the cause of the sharp peaks at 68° E and 72° E in the gray shade curve. At 0600 GMT, the gray shades are, in general, lower and the variations in gray shade are attributable to orography. The orographic effects are clearly reflected by the nature of the variation at other times.

**80° to 86° E**— The region between 75° and 80° E has uniform gray shade throughout the day with little spatial variation mostly because of permanent snow cap. This is in contrast with the steep and irregular variation observed over 80° to 86° E segment. Since this segment is over the western part of the Tibetan plateau which is without much undulations, the gray shade variations are attributable to the presence of low clouds which is in fact confirmed from satellite pictures. At 0600 GMT, the warm land surface of the plateau is distinguishable in cloud-free areas. Between 86° and 91° E the plateau is generally cloud-free and gray shade values are quite uniform.

**95° to 100° E**— Although this is a region of pronounced variations in terrain height, the gray shade variations are most intense only at 0600 GMT where orographic effects are accentuated by isolated patches of low clouds.

**28° to 30° N**— This segment runs across the Himalayas which are the cause of steep variations in gray shade at 0600 GMT.

**34° to 42° N**— The cold and cloudy peaks of the Kunlun to the north of the Tibetan plateau are evident from the high gray shades in the middle of this segment. Further north over Sinkiang, which is at a much lower elevation, the gray shades are again lower.

**North of 45° N**— Convective clouds were present at 1200 GMT and 1800 GMT masking the effects of orography which are noticeable only at 0600 GMT. It must be borne in mind that the gray shade—temperature relationship is not linear (Fig. 1). Hence, a large variation in gray shade may correspond to a small variation in the temperature over the middle segment of the curve, *i.e.*, when the gray shade is between 16 and 150.

### 3.3. Temperature contours

From the radiance data of the four selected images, temperature contours were plotted with the help of DAID on a region bounded by 20° to 50° N and 70° to 105° E approximately. These are reproduced in Figs. 6 to 9. However, some unnecessary details have been omitted therein to bring out the essential features more clearly. The term temperature is used here in the sense defined by Eqn. (1). The actual surface temperature  $T_{sfc}$  or cloud top temperature when the surface is obscured, will be higher than the satellite-derived one,

$$T_{sfc} = T_B + \Delta T \quad (2)$$

because (i) the emissivity of the surface may be less than one, and (ii) the atmospheric column may not be totally transparent in the 10.5–12.5  $\mu$  region, but have some attenuating effect. The second term in Eqn. (2), *i.e.*,  $\Delta T$  is about 1–2° K at  $T_{sfc} = 260^\circ$  K and increases to a value of 6–8° K at  $T_{sfc} = 300^\circ$  K (Gupta 1978). However, since the bulk of the water vapour resides in the lower troposphere the attenuation errors in the temperature estimation are negligible for middle and high clouds and for highly elevated terrain like the Tibetan plateau. The IR emissivity values of different types of surface are very close to 1.0, varying between 0.95 for sand, 0.986 for thick green grass, 0.996 for dry snow and 0.998 for water (Kondratyev 1972).

The 1200 GMT (local evening) pattern (Fig. 6) shows that most of the Tibetan plateau and the Tien Shan mountain range have  $T_B$  values of 275° to 300° K. These are comparable to  $T_B$  values over the desert plains of Takla Makan and Gobi. The cold pools (225°K) lying over the Himalayas and to the south of them are attributable to high and tall clouds.

The 1800/0000 GMT (local night/local morning) patterns (Figs. 7 and 8) show that  $T_B$  is of the order of 250 to 275°K over most of the elevated region. In fact, the 275° K isotherm at 0000 GMT almost coincides with the orographic contour shown in Fig. 3, with lower values persisting to the north and south of it. Because of cloudiness, temperature of 225° K persists over the Gangetic plains. Again, temperatures above 275° K are observed over large parts of the Tibetan plateau and the desert areas. The 0600 GMT (local noon) contours (Fig. 9) show very explicitly the warming of the Tibetan plateau. The 275° K isotherm is seen to be pushed much to the south pointing to an increase in the extent of the warm area. A large area of the plateau is warmer than 300° K and  $T_B$  is greater than 310° K in the core of the warm area. The deserts have the same order of temperature.

It is very often argued that although the pattern of variation of a satellite-derived parameter can be considered reliable, the absolute value of that parameter cannot be taken for granted. From this point of view, whatever surface temperature observation were available over Tibet (Table 2) were plotted for comparison with  $T_B$  values (Figs. 6 to 9).  $T_B$  values are seen to be very closely agreeing with the surface observation at 0600 GMT (Fig. 9) and 1200 GMT (Fig. 6). Whereas during night time (Figs. 7 and 8), at some stations, the recorded temperatures are a few degrees higher than  $T_B$  which tend to be around 275°K. These differences which are within the range of  $\Delta T$  discussed earlier are due to local effects not representative of the surrounding areas.

### 4. Conclusion

This study based on the short period data obtained from INSAT-1A has demonstrated that the Tibetan plateau region was considerably warmer during an active monsoon situation over India. A detailed study with data spanning over different phases of a

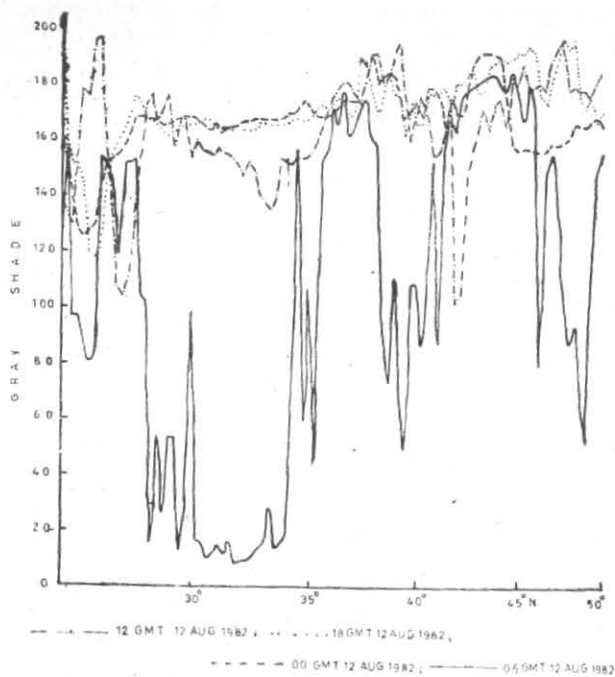


Fig. 5



Fig. 6

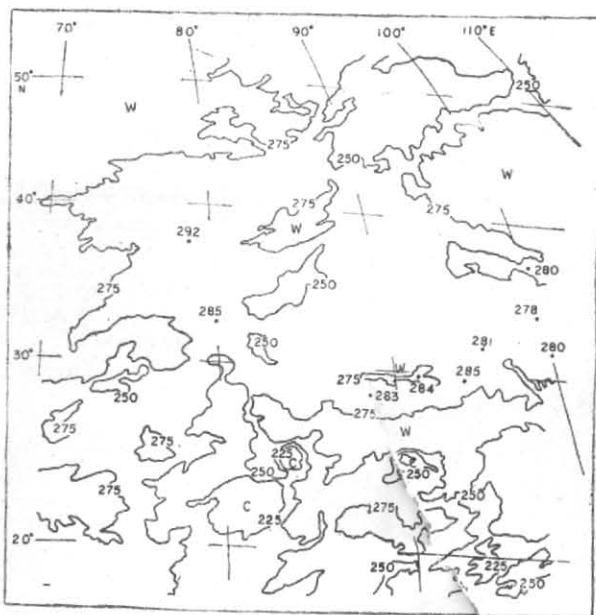


Fig. 7

TABLE 2  
Coordinates of stations in the Tibetan region

Station	Latitude (Deg. Min. N)		Longitude (Deg. Min. E)		Height (metres)
Tingri	28°	38'	87°	05'	4302
Deqin	28	39	99	10	3591
Jiulon	28	59	101	33	2994
Xigaze	29	30	88	55	3837
Nyingachi	29	33	94	21	3001
Lhasa	29	42	91	08	3650
Batang	30	05	98	55	2589
Dengoin	31	25	95	36	3874
Nagqu	31	29	92	03	4508
Ganzi	31	38	99	59	3394
Gar	32	30	80	05	4279
Yushu	33	06	98	45	3704
Tuotuohe	33	37	99	59	3394
Darlag	33	48	99	48	3968
Mado	34	57	98	08	4221
Tongde	35	09	100	20	3290
Lanzhou	36	03	103	53	1518
Germu	36	12	94	38	2809
Dulan	36	20	98	02	3192
Xining	36	45	101	36	2296
Gangca	37	20	100	10	3301
Pishan	37	37	78	17	1376
Da-Qaidan	37	50	95	17	3174
Mangya	37	56	83	39	1264
Jiuquan	39	46	98	31	1478



Fig. 8



Fig. 9

monsoon season would be very useful to show the variations in the warm source region of the Tibetan plateau. It is hoped that INSAT-1B will provide an opportunity to monitor the Tibetan region continuously. This would help to analyse the role of the plateau during the onset of the monsoon and to establish any linkage between the intensity of the warming and the activity of the monsoon.

#### References

- Chin, P.C. and Lai, M.H., 1974, "Monthly mean upper winds and temperatures over Southeast Asia and the Western North Pacific", Hong Kong Royal Observatory Tech. Memo. No. 12, 115 pp.
- Flohn, H., 1958, "Recent investigation on the mechanism of the summer monsoon of Southern and Eastern Asia", *Proc. Symp. Monsoons of the World*, New Delhi, pp. 75-88.
- Godbole, R.V., Kelkar, R.R. and Murakami, T., 1970, "Radiative equilibrium temperature of the atmosphere along 80°E longitude", *Indian J. Met. Geophys.*, **21**, pp. 43-52.
- Godbole, R.V., 1973, "Numerical simulation of the Indian summer monsoon", *Indian J. Met. Geophys.*, **24**, pp. 1-14.
- Gupta, R.K., 1978, "Infrared remote temperature measurement, its physics, etc.", *J. Indian Inst. Sci.*, **60**, pp. 135-169.
- Kelkar, R.R., 1970, "Role of radiation in atmospheric circulation", Ph. D. thesis, Univ. of Poona, 241 pp.
- Kondratyev, K. Ya., 1972, "Radiative processes in the atmosphere", WMO No. 309, 214 pp.
- Koteswaram, P., 1958, "The Asian summer monsoon and the general circulation over the tropics" *Proc., Symp. Monsoons of the World*, New Delhi, pp. 105-110.
- Staff Members, Academia Sinica, 1958, "On the general circulation over Eastern Asia", Part II, *Tellus*, **10**, pp. 58-75.